HHS Public Access

Author manuscript

Circ Res. Author manuscript; available in PMC 2016 October 09.

Published in final edited form as:

Circ Res. 2015 October 9; 117(9): 804–816. doi:10.1161/CIRCRESAHA.115.306886.

Wnt10b Gain-of-Function Improves Cardiac Repair by Arteriole Formation and Attenuation of Fibrosis

David T. Paik[1,2], **Meena Rai**[1,2], **Sergey Ryzhov**[1,4], **Lehanna N. Sanders**[1,2], **Omonigho Aisagbonhi**[1,2,5], **Mitchell J. Funke**[1,6], **Igor Feoktistov**[1,3], and **Antonis K. Hatzopoulos**[1,2]

[1]Department of Medicine, Division of Cardiovascular Medicine, Vanderbilt University, Nashville, TN U.S.A

[2]Department of Cell and Developmental Biology, Vanderbilt University, Nashville, TN U.S.A

[3]Department of Pharmacology, Vanderbilt University, Nashville, TN U.S.A

[4]Center for Molecular Medicine, Maine Medical Center Research Institute, Scarborough, ME, U.S.A

[5]Department of Pathology, Harvard Medical School, Massachusetts General Hospital, Boston, MA, U.S.A

[6]Golden Rule Medical, Cincinnati, OH, U.S.A

Abstract

Rationale—Myocardial infarction causes irreversible tissue damage, leading to heart failure (HF). We recently discovered that canonical Wnt signaling and the Wnt10b ligand are strongly induced in mouse hearts after infarction. Wnt10b regulates cell fate in various organs, but its role in the heart is unknown.

Objective—To investigate the effect of Wnt10b gain-of-function on cardiac repair mechanisms and assess its potential to improve ventricular function after injury.

Methods and Results—Histological and molecular analyses showed that Wnt10b is expressed in cardiomyocytes and localized in the intercalated discs of mouse and human hearts. After coronary artery ligation or cryoinjury in mice, Wnt10b is strongly and transiently induced in peri-infarct area cardiomyocytes during granulation tissue formation. To determine the effect of Wnt10b on neovascularization and fibrosis, we generated a mouse line to increase endogenous Wnt10b levels in cardiomyocytes. We found that gain of Wnt10b function orchestrated a recovery phenotype characterized by robust neovascularization of the injury zone, less myofibroblasts, reduced scar size, and improved ventricular function compared to wild-type mice. Wnt10b stimulated expression of Vascular Endothelial Growth Factor Receptor 2 (Vegfr-2) in endothelial cells and Angiopoietin-1 in vascular smooth muscle cells through NF-κB activation. These effects

Address correspondence to: Dr. Antonis K. Hatzopoulos, Vanderbilt University, Department of Medicine, Division of Cardiovascular Medicine, Nashville, TN 37232-6300, Tel: (615) 9365529, FAX: (615) 9361872, antonis.hatzopoulos@vanderbilt.edu.

DISCLOSURES

The authors declare no competing financial interests.

coordinated endothelial growth and smooth muscle cell recruitment, promoting robust formation of large, coronary-like blood vessels.

Conclusion—Wnt10b gain-of-function coordinates arterial formation and attenuates fibrosis in cardiac tissue after injury. Because generation of mature blood vessels is necessary for efficient perfusion, our findings could lead to novel strategies to optimize the inherent repair capacity of the heart and prevent the onset of HF.

Keywords

Endothelial cell growth; angiogenesis; fibrosis; Wnt signaling; Wnt10b; NF-κB

INTRODUCTION

Coronary heart disease leading to myocardial infarction (MI) is the major cause of death in both men and women. Each year about 735,000 people in the U.S. have an MI and suffer tissue damage, often leading to ventricular remodeling, hypertrophy, dilatation and heart failure (HF).[1,2]

Cardiomyocytes within the infarct area die within minutes after coronary artery occlusion.[3,4] Toxic products and alarm signals released from dying cells induce cell adhesion proteins, cytokines and chemokines to recruit inflammatory cells, which remove cellular debris and degrade extracellular matrix.[5–7] After debris is cleared, usually within 2–3 days after MI, the gap is filled with granulation tissue composed of proliferating myofibroblasts that secrete extracellular matrix proteins and endothelial cells that form new capillaries.[6–8] Two to three weeks after the original MI, the infarcted tissue begins to mature into a dense scar.[8] Despite considerable progress to restore circulation to infarcted areas using thrombolytics and percutaneous interventions, we currently have no pharmaceutical agents to modulate endogenous cardiac repair processes with the goal of preserving left ventricular (LV) function and preventing HF.

We and others have demonstrated that canonical Wnt signaling is activated in myofibroblasts and endothelial cells during granulation tissue formation following experimental MI in mice, suggesting that the Wnt pathway plays a role in both angiogenesis and fibrosis.[9–13] Our results further showed that Wnt10b, a canonical Wnt ligand, is induced after MI.[12] Although previous studies in animal models have shown that modulation of Wnt antagonists such as Sfrp1 and intracellular downstream targets such as β-catenin can influence the wound healing process after MI, the effects of canonical Wnt ligands such as Wnt10b on cardiac tissue repair have not been investigated.[9,10,14,15]

To determine the effects of Wnt10b on the cardiac repair process, we analyzed the spatial and temporal patterns of Wnt10b activation in the heart before and after injury. We discovered that in normal human and mouse hearts, Wnt10b is expressed in cardiomyocytes and stored in the intercalated discs. Following ventricular tissue injury in mice, Wnt10b expression is strongly and transiently up-regulated in cardiomyocytes around the injury, peaking during granulation tissue formation. Our results show that Wnt10b gain-of-function in cardiomyocytes leads to i) increased angiogenesis both directly by stimulation of

endothelial cell proliferation and by induction of Vegfr2 expression, ii) formation of coronary-like vessels surrounded by vascular smooth muscle cells (vSMCs) via induction of Ang-1 in vSMCs, iii) cardiomyogenesis within scar tissue and iv) decreased numbers of myofibroblasts and infiltrating inflammatory cells. Furthermore, we show that the mechanisms underlying arteriole formation by Wnt10b depend on coordinated stimulation of the NF-κB signaling pathway in endothelial cells and vSMCs. These findings suggest Wnt10b has the potential to orchestrate and improve the natural reparative capacity of the heart.

METHODS

A complete Methods section is available in the Online Data Supplement.

RESULTS

Wnt10b is expressed in cardiomyocytes and localized in the intercalated discs

To identify the cell types expressing WNT10B protein in the adult human heart, we stained tissue sections from healthy heart donors with an antibody recognizing the N-terminal domain of WNT10B. Immunofluorescence (IF) analysis showed that WNT10B was localized in the intercalated discs of cardiomyocytes, co-localizing with β-catenin (CTNNB1) and Connexin 43 (GJA1; Figure 1A). In contrast, we detected abundant cytoplasmic staining and WNT10B accumulation along the lateral borders of cardiomyocytes in ventricular tissue from ischemic cardiomyopathy patients (Figure 1B). Using a distinct antibody against the C-terminal protein domain of Wnt10b,[16] we found similar accumulation in the intercalated discs of the mouse heart (Fig 1C). Western blot analysis of protein samples prepared from freshly isolated cardiomyocytes confirmed myocyte-specific Wnt10b expression (Online Figure I).

Wnt10b is induced in cardiomyocytes at the infarct border during granulation tissue formation

To determine the spatio-temporal pattern of Wnt10b expression in the heart after injury, we induced MI in C57BL/6 adult mice by permanent ligation of the left coronary artery and analyzed whole heart RNA samples at specific time points of the cardiac tissue repair process. Specifically, we quantified *Wnt10b* levels during the inflammatory response phase (day 1 to 3 after injury), granulation tissue formation (i.e., during neovascularization and fibrosis after day 4) and in mature scar at day 21 in comparison to baseline levels. Our results showed *Wnt10b* RNA levels began to rise around day 3 post MI, peaking at day 7 by 6–8 fold, but returning to baseline levels during scar maturation (Figure 1D). *Wnt10b* peak levels followed the induction of TGFβ1 that is known to promote granulation tissue formation and fibrosis (Figure 1D).[17]

To identify the location of Wnt10b induction in the heart after injury, we analyzed mouse cardiac tissue sections on day 2 and 7 post MI. While little to no change in Wnt10b protein localization was detected at day 2 post MI (Online Figure I), we observed strong induction of Wnt10b protein specifically in the myocytes of the infarct border zone at day 7 post MI (Figure 1E and 1F). In addition to the intercalated disc localization in normal hearts or in

cardiomyocytes remote from the infarct, Wnt10b accumulated prominently in the cytoplasm of border zone cardiomyocytes (Figure 1E and 1F).

Taken together, our data show that Wnt10b protein localizes in the intercalated discs of cardiomyocytes in the normal adult heart. This pattern is disturbed in ischemic cardiomyopathy patients with cytoplasmic accumulation of WNT10B. Moreover, Wnt10b protein is strongly increased in peri-infarct cardiomyocytes during the neovascularization and fibrosis phase of cardiac repair after experimental MI.

Wnt10b gain-of-function promotes functional recovery after injury

To determine whether Wnt10b gain-of-function is beneficial or detrimental to cardiac repair, we genetically enhanced the natural Wnt10b expression in cardiomyocytes by generating a transgenic mouse line carrying the entire *Wnt10b* coding sequence under the adult cardiomyocyte-specific *alpha Myosin Heavy chain* (*αMHC* or *Myh6*) gene promoter (Figure 2A).[18] Molecular analyses of ventricular tissue showed that *αMHC-Wnt10b* transgenic (TG) mice expressed higher levels of *Wnt10b* RNA and Wnt10b protein in the heart compared to wild-type (WT) controls; however, Wnt10b protein in TG was primarily localized in the intercalated discs, as in WT cardiomyocytes (Figure 2B and Online Figure II). Wnt10b overexpression did not cause changes in the ventricles of TG mice at the macroscopic or ultrastructural level, but it led to enlargement of both atria (Online Figure II). TG mice displayed normal ventricular dimensions and functional parameters compared to WT controls (Online Table I). Flow cytometry of primary non-myocyte cells isolated from adult WT and TG ventricles also showed comparable numbers of immune, endothelial and stromal cells (Online Figure III).

Because the enlarged atria of TG mice hindered ligation of coronary vessels, we assessed the effects of Wnt10b overexpression on cardiac tissue repair using the cryoinjury model.[19,20] Histological and molecular analyses of Wnt10b expression after cryoinjury showed induction at day 7 after injury that was confined to cardiomyocytes in the injury border zone, as observed in the MI model, suggesting that both spatial and temporal Wnt10b expression patterns are comparable in the two injury models (Online Figure IV).

Cardiac functional parameters were measured by echocardiography at baseline before injury, and at 1 day, 1 week and 3 weeks after injury (Figure 2C–E). The results showed that the extent of the initial injury was similar in WT and TG mice as demonstrated by similar drops in fractional shortening (FS) 1 day after injury. However, whereas the function of WT hearts continued to deteriorate over time, left ventricular functional output of TG hearts improved 3 weeks after injury (Figure 2C). Functional recovery in TG mice was primarily due to preservation of systolic function, with preserved chamber size and contractility (Figure 2D and 2E). Improved cardiac function in TG mice matched attenuated induction of prognostic markers of HF, such as Matrix Metalloproteinase-9 (*Mmp9*)[21–23] and atrial and brain natriuretic peptides (*Nppa, Nppb*),[22,24,25] when compared to WT counterparts (Figure 2F).

Consistent with the echocardiography data, histological analysis demonstrated that the original injury size was comparable in WT and TG mice. By 3 weeks post injury, however, TG ventricles displayed reduced scar than WT counterparts, with attenuated deposition of

collagen 1A (Figure 2G and 2H). The injured tissue in TG ventricles instead contained numerous patches of α-Actinin^{+} myocytes with developing sarcomeric structures (Figure 2I and 2J). Together, our data suggest Wnt10b has a favorable effect on cardiac repair, leading to reduced scar size, cardiomyocyte generation, improved systolic function and reduction in the expression of HF markers.

Wnt10b overexpression increases neovascularization of scar tissue

To test the effect of Wnt10b on cardiac tissue repair, we compared scar neovascularization and myofibroblast accumulation between WT and TG mice after cryoinjury. Histological and flow cytometry analyses showed that ventricles of uninjured WT and TG mouse hearts contained comparable numbers of endothelial cells (Online Figure V). After injury, IF analysis using the CD31 antibody to mark endothelial cells showed the presence of small and sparse microcapillaries within the injured tissue of WT hearts, as previously reported.[20] In contrast, the corresponding injured tissue in TG ventricles contained more vascular beds than WT, organized in dense vascular regions or as large-diameter blood vessels (Figure 3A). Vascular density of tissue away from the site of injury was comparable in WT and TG mice, whereas the injured tissue of TG ventricles was approximately 2-fold more densely vascularized than the corresponding area in WT counterparts (Figure 3A). Consistent with the histology data, flow cytometry analysis of dissociated total ventricular tissues showed TG hearts to contain approximately 30% more endothelial cells (CD31^{+}αSMA^{-}) than WT (Figure 3B, Online Figure V).

We found Wnt10b overexpression had the opposite effect on the number of myofibroblasts generated after injury (Figure 3C–E). Flow cytometry showed ventricles of uninjured WT and TG mice contained comparable numbers of CD31^{-}CD140a^{+} fibroblasts (Online Figure V). After injury, the number of total fibroblasts in WT and TG mice remained comparable. We observed a significant increase in the number of myofibroblasts in both WT and TG ventricles as expected, though TG ventricles contained approximately half the number of αSMA^{+}, collagen-producing myofibroblasts compared to WT (Figure 3C–E, Online Figure V).

IF analysis with a nuclear proliferation marker Ki-67 showed the majority of proliferating cells within the injured tissue of TG ventricles were endothelial cells (Figure 3F). In contrast, most Ki-67^{+} cells within the injured tissue in WT ventricles were non-endothelial cells (Figure 3F, Online Figure V). Flow cytometry quantified that the ratio of endothelial to non-endothelial Ki-67^{+} cells was 2.5 higher in TG mice compared to WT counterparts (Figure 3G). These data indicate that Wnt10b promotes proliferation of endothelial cells at the expense of non-endothelial cells, which in the case of the injured tissue are mostly myofibroblasts.[8]

Wnt10b gain-of-function in cardiomyocytes induces canonical Wnt signaling in adjacent endothelial cells, increasing their proliferative capacity

Analysis of RNA from TG ventricles prior to injury showed Wnt10b gain-of-function led to up-regulation of canonical Wnt signaling target genes *Axin2, Lef1* and *Tcf7* (Figure 4A).[26–28] To identify the cell types with canonical Wnt activation in TG hearts, we stained

cardiac tissue sections with an antibody recognizing the canonical Wnt signaling molecule β-catenin. IF analysis showed accumulation of β-catenin in endothelial cells, but not in cardiomyocytes, indicating Wnt10b overexpression activated canonical Wnt signaling in endothelial cells in a paracrine fashion (Figure 4B). Furthermore, transfection of freshly isolated cardiac endothelial cells with canonical Wnt activity luciferase reporter constructs confirmed higher canonical (i.e., β-catenin-mediated) Wnt signaling in cells from TG mice compared to those from WT mice (Figure 4C).

To test whether canonical Wnt activity promotes the proliferative capacity of endothelial cells, we purified and cultured freshly isolated endothelial cells from WT and TG ventricles (Online Figure VI). Our data show endothelial cells from TG ventricles possessed higher growth potential in culture and branching morphogenesis on Growth Factor Reduced (GFR) Matrigel than endothelial cells isolated from WT ventricles (Fig 4D–G). This effect was abolished when endothelial cells were treated with the small molecule canonical Wnt inhibitor IWR-1-*endo*,[29] but not the JNK inhibitor SP600125,[30] demonstrating that the high growth potential of cardiac endothelial cells isolated from TG ventricles was due to elevated canonical Wnt activity (Figure 4H and 4I).

Wnt10b enhances endothelial cell growth both directly and through induction of Vegfr-2 expression

To test whether the high growth potential of endothelial cells isolated from TG ventricles was a direct effect of Wnt10b on endothelial cells, we isolated cardiac microvascular endothelial cells from WT mice and exposed them to increasing concentrations of recombinant Wnt10b protein, which induced canonical Wnt activity (Online Figure VII). Wnt10b protein directly promoted endothelial cell growth in culture, suggesting canonical Wnt activity induction and stimulation of endothelial cell proliferation was a direct effect of Wnt10b (Figure 5A, Online Figure VII).

The Vegf-a/Vegfr-2 ligand/receptor axis specifically regulates endothelial cell proliferation.[31,32] As shown in Figure 5B, Wnt10b induced *Vegfr-2* in addition to the canonical Wnt gene target *Axin2* in cultured endothelial cells, indicating that Wnt10b can further enhance the response of endothelial cells to Vegf-a by increasing the levels of its receptor. To test this possibility, we analyzed the effect of Vegf-a in vascular tube formation in the presence or absence of Wnt10b. We found Wnt10b and Vegf-a cooperated in stimulating endothelial tube formation *in vitro* (Figure 5C). These findings indicate Wnt10b both directly stimulates endothelial cell growth and amplifies the pro-angiogenic effects of Vegf-a by induction of *Vegfr-2*.

Wnt10b promotes formation of mature coronary-like blood vessels

In addition to greater density, the vasculature within injured tissue of TG hearts consisted of large-diameter blood vessels, in contrast to small-diameter capillaries present in WT hearts (Figure 3A). Co-staining with antibodies recognizing endothelial and vSMCs confirmed scar tissue in TG mice contained greater number of blood vessels surrounded by a prominent smooth muscle cell layer, as compared to that in WT (Figure 6A).

To identify the molecular basis of the observed vascular phenotype, we measured expression of Ang-1 and its receptor Tie2, which regulate vSMCs recruitment and blood vessel stability.[33,34] Analysis of ventricle tissue RNA of WT and TG mouse hearts showed comparable baseline Ang-1, Ang-2 and Tie2 expression levels prior to injury. However, there was a strong (15-fold) induction of Ang-1 expression 1 week after injury in WT ventricular tissue, which was further increased by 2-fold in TG ventricles (Figure 6B). In contrast, there were no major differences in the expression of Tie2 and the Ang-1 antagonist Ang-2 between WT and TG tissue (Figure 6B). Histological analysis pointed to higher Ang-1 levels in αSMA^+ cells surrounding blood vessels within TG scar tissue compared to WT controls (Figure 6C).

To test whether Wnt10b-induced arteriole morphogenesis is due to activation of the Ang/Tie2 signaling axis, we co-cultured endothelial and vSMCs with or without Wnt10b and a Tie2 kinase-specific inhibitor.[35] We found Wnt10b induced association of endothelial and smooth muscle cells in GFR Matrigel. Moreover, Tie2 inhibition abolished Wnt10b-induced endothelial/smooth muscle cell interactions (Figure 6D). Taken together, our results indicate Wnt10b promotes vSMCs recruitment and blood vessel stability by activating the Ang-1/Tie2 pathway.

Wnt10b orchestrates vessel stabilization through coordinate induction of NF-κB signaling in endothelial and smooth muscle cells

Previous studies have identified NF-κB and Notch signaling as critical pathways in arteriogenesis, collateral vessel formation and vascular network size during development, or in the adult through coordinate promotion of angiogenesis and vSMC recruitment.[36–38] We observed no significant differences in Notch signaling targets such as Hey1 and Hey2 after injury between WT and TG mice (Online Figure VIII). To test whether Wnt10b acts upstream of the NF-κB signaling pathway, we investigated its effect on NF-κB signaling activation. Our data show Wnt10b treatment of endothelial and smooth muscle cells, transfected with NF-κB luciferase reporter constructs, led to induction of NF-κB signaling in both cell types (Figure 7A and 7B). The NF-κB signaling activation effect was Wnt10b-specific, since the non-canonical Wnt11 ligand, which is also strongly induced in the heart after injury,[12] had only a moderate effect. No synergistic interaction was observed between Wnt10b and TNFα-induced NF-κB signaling in endothelial cells even at low TNFα concentrations (Online Figure VIII).

To test whether the effect of Wnt10b on the induction of genes regulating endothelial cell growth (*Vegfr-2*) and vSMC recruitment (*Ang-1*) genes was due to activation of NF-κB signaling, we incubated endothelial and smooth muscle cells with Wnt10b in the presence or absence of the NF-κB signaling inhibitor SN50.[39] The results show Wnt10b-mediated induction of *Vegfr-2* in endothelial cells and *Ang-1* in smooth muscle cells was abolished by SN-50 (Figure 7C and 7D). Furthermore, Wnt10b also induced *Pdgf-b* expression in endothelial cells in a NF-κB-dependent manner. Pdgf-b is known to act on Pdgfr-β receptor, expressed in vSMCs, to promote recruitment to newly formed blood vessels.[40]

Previous studies have shown that leaky blood vessels hinder tissue recovery because they allow infiltration of immune cells resulting in unresolved inflammation, which in turn may

aggravate ventricular remodeling.[6] This raised the possibility that Wnt10b-induced blood vessel stability attenuates inflammation. Consistent with this possibility, flow cytometry analysis 5 days after cryoinjury showed lower levels of inflammatory cells within ventricular tissue of TG mice compared to WT (Figure 7E and 7F, Online Figure IX).

Consequently, our data indicate Wnt10b promotes angiogenesis and blood vessel stabilization through parallel stimulation of NF-κB signaling in endothelial and smooth muscle cells, a pathway that is known to regulate induction of pro-angiogenic and arteriogenic factors in endothelial cells (Figure 8).[36,37,39,41] The coordinated formation of stable blood vessels improves perfusion of injured tissue and prevents prolonged infiltration of inflammatory cells, creating an optimized microenvironment for cardiomyocyte growth and enhanced repair of injured cardiac tissue.

DISCUSSION

Here we show canonical Wnt signaling activating Wnt10b ligand is expressed in cardiomyocytes and stored in intercalated discs. After injury, Wnt10b expression is induced in cardiomyocytes in border zone during the granulation tissue formation phase of cardiac repair, when neovascularization and fibrosis take place. Our data show that Wnt10b gain-of-function stimulates new blood vessel growth in two separate ways. First, Wnt10b activates canonical Wnt signaling in endothelial cells, a process that is known to promote angiogenesis after myocardial injury.[42] Second, by stimulating Vegfr-2 expression in endothelial cells, Wnt10b further enhances Vegf-a-mediated endothelial cell proliferation.

Furthermore, Wnt10b mediates stable vessel formation via induction of Pdgf-b expression in endothelial cells and Ang-1 in smooth muscle cells, two growth factors that promote vascular stabilization, reduce permeability and enhance blood flow.[40,43,44] Previous studies have established that simultaneous supply of VEGF and Ang-1 leads to superior functional neovascularization of ischemic tissues while administration of VEGF alone generates leaky vessels and hemorrhages.[45–47] Although such secreted factors regulating individual aspects of blood vessel formation have been identified, knowledge of upstream regulators that coordinate the entire process was missing. To our knowledge, Wnt10b is the first morphogen that coordinates coronary-like vessel formation, pointing to new approaches to effectively re-vascularize poorly perfused areas of the heart. However, future studied will need to address the mechanisms leading to atria enlargement as a potential negative effect caused by Wnt10b overexpression.

Formation of large blood vessels with robust support structures involves endothelial cell growth, branching and recruitment of smooth muscle cells.[43] In support of our data on the role of Wnt10b in adult cardiac repair, it was recently shown that endothelial transcription factor ERG promotes vascular stability and growth through canonical Wnt activation during development.[48] Previous studies have also identified the NF-κB pathway, Notch signaling, RAF-1/ERK and the adaptor protein Shc as intracellular components that coordinate arteriogenesis, collateral vessel formation and vascular network size during development or in the adult.[36–38] Although we did not detect changes in Notch signaling in TG mouse hearts, we discovered that Wnt10b activated NF-κB signaling in both cardiac endothelial

and smooth muscle cells. It is thus likely that coordinated activation of NF-κB signaling in both cell types mediating vessel growth and stability is responsible for the Wnt10b effects. In support of this notion, we found inhibition of NF-κB signaling abolished Wnt10b-induced expression of *Vegfr-2* and *Ang-1* in endothelial and smooth muscle cells, respectively. Links between Wnt and NF-κB signaling have also been identified in osteosarcoma cells and hair follicle formation,[49,50] suggesting the cross-talk between the two pathways has broader roles in development and disease.

The effects of Wnt10b on neovascularization of the injured tissue led to significant restoration of ventricular function after injury, as evidenced by improved systolic parameters, reduced infarct size and attenuated expression of HF biomarkers in TG mice. This recovery phenotype mimics that of mice with sustained Ang-1 treatment, which promoted vessel size expansion and increased the diameter of arterioles, suggesting Wnt10b acts upstream of the Angiopoietin/Tie2 signaling axis.[46] Furthermore, Wnt10b promoted formation of cardiac tissue within scar, which may further account for the improved ventricular function. This result would be consistent with findings showing that canonical Wnt signaling activation promotes cardiomyocyte proliferation in the embryonic heart.[51] Finally, Wnt10b gain-of-function led to decreased numbers of collagen-producing myofibroblasts and infiltrating pro-inflammatory cells, although further studies are needed to test whether this is a direct Wnt10b effect on these cells types. At present it is not clear if these responses reflect direct effects of Wnt10b on myofibroblast or cardiomyocyte proliferation, expansion and differentiation of cardiac progenitor cells, or regulation of cell fates during endothelial-to-mesenchymal (EndMT) or mesenchymal-to-endothelial (MEndT) transitions[7,12,52–54]

Interestingly, Wnt pathway antagonists such as sFRPs also have positive effects in cardiac repair because they stimulate early cell survival through Akt-1 activation.[9,10,14,55] In contrast, activation of canonical Wnt signaling in myofibroblasts accelerated scar formation, benefiting recovery as shown in mice with constitutive fibroblast expression of β-catenin.[13,56] It would be important to test whether stage-, ligand- and cell-specific manipulation of Wnt signaling could further optimize the recovery process.

A limitation of the Wnt10b gain-of-function approach in our study is that the observed phenotypes may not only recapitulate the endogenous role of Wnt10b, but also reflect the collective overexpression effects of structurally related Wnt ligands in the heart. This problem is particularly acute in the Wnt signaling pathway, which consists of 19 ligands and 10 frizzled receptors with overlapping, often redundant expression and function.[57,58] However, it is noteworthy that the observed phenotypes are distinct from those described in *αMHC*-Wnt11 transgenic mice, which displayed cardiomyopathy due to hypertrophic ventricular myocytes,[59] suggesting that, at least part of the results are specific to the Wnt10b ligand. Thus, development of Wnt10b administration protocols, or compounds designed to mimic Wnt10b, will likely help orchestrate stable blood vessel formation after injury, improve cardiac tissue recovery, and potentially decrease ventricular remodeling and heart failure.

Supplementary Material

Refer to Web version on PubMed Central for supplementary material.

Acknowledgments

We thank the Cardiovascular Pathophysiology & Complications Core of the Mouse Metabolic Phenotyping Center, the Cell Imaging Shared Resource (supported by NIH grants CA68485, DK20593, DK58404, HD15052, DK59637 and EY08126), the Translational Pathology Shared Resource, the Transgenic Mouse/ES Cell Resource, Molecular Cell Biology Resource, and the FACS Core at Vanderbilt University Medical Center. We thank Lianli Ma and Zhizhang Wang for performing mice surgeries and echocardiograms, and Douglas Sawyer and Chee Lim for providing freshly isolated cardiomyocytes.

SOURCES OF FUNDING

This work was supported by NIH grants HL083958 and HL100398 to A.K.H., HL095787 to I.F., and Institutional Support from Vanderbilt University Medical Center to A.K.H.; a Program in Cardiovascular Mechanisms: Training in Investigation fellowship (T32HL007411) to D.T.P. and L.N.S.; HHMI/VUMC Certificate Program in Molecular Medicine to D.T.P.; NIGMS grant T32GM07347 to Vanderbilt MSTP; and an American Heart Association pre-doctoral Fellowship to O.A.

Nonstandard Abbreviations and Acronyms

αMHC	alpha Myosin Heavy Chain (Myh6)
αSMA	alpha Smooth Muscle Actin
Ang-1	2, Angiopoietin-1, Angiopoietin-2
CD31	Cluster of differentiation 31, or Platelet Endothelial Cell Adhesion Molecule-1
FS	Fractional Shortening
GAPDH	Glyceraldehyde-3-phosphate dehydrogenase
GFR	Growth Factor Reduced (Matrigel)
HF	Heart failure
IF	Immunofluorescence
JNK	c-Jun N-terminal Kinase
Lef1	Lymphoid Enhancer-binding Factor 1
MI	Myocardial infarction
MMP	Matrix metalloproteinase
NF-κB	Nuclear Factor kappa-light-chain-enhancer of activated B cells
Pdgf-b	Platelet-Derived Growth Factor subunit B
Pdgfrβ	Platelet-Derived Growth Factor Receptor beta
Tie2	Tyrosine kinase with immunoglobin-like and EGF-like domains 2
Tcf7	Transcription Factor 7
Vegf-a	Vascular Endothelial Growth Factor-A
Vegfr-2	Vascular Endothelial Growth Factor Receptor 2 (Flk-1 or KDR)

References

1. Mozaffarian D, Benjamin EJ, Go AS, et al. Heart disease and stroke statistics—2015 update: a report from the American Heart Association. Circulation. 2015; 27:e29–322. [PubMed: 25520374]
2. Braunwald E. The war against heart failure: the Lancet lecture. Lancet. 2015; 385:812–24. [PubMed: 25467564]
3. Konstantinidis K, Whelan RS, Kitsis RN. Mechanisms of cell death in heart disease. Arterioscler Thromb Vasc Biol. 2012; 32:1552–62. [PubMed: 22596221]
4. O'Neal WT, Griffin WF, Kent SD, Virag JAI. Cellular pathways of death and survival in acute myocardial infarction. J Clin Exp Cardiolog. 2012; S6:003.
5. Timmers L, Pasterkamp G, de Hoog VC, Arslan F, Appelman Y, deKleijn DPV. The innate immune response in reperfused myocardium. Cardiovasc Res. 2012; 94:276–83. [PubMed: 22266751]
6. Frangogiannis NG. The inflammatory response in myocardial injury, repair, and remodelling. Nat Rev Cardiol. 2014; 11:255–65. [PubMed: 24663091]
7. Boudoulas KD, Hatzopoulos AK. Cardiac repair and regeneration: the Rubik cube of cell therapy for heart disease. Dis Model Mech. 2009; 2:344–58. [PubMed: 19553696]
8. Virag JI, Murry CE. Myofibroblast and endothelial cell proliferation during murine myocardial infarct repair. Am J Pathol. 2003; 163:2433–40. [PubMed: 14633615]
9. Barandon L, Couffinhal T, Ezan J, Dufourcq P, Costet P, Alzieu P, Leroux L, Moreau C, Dare D, Duplaa C. Reduction of infarct size and prevention of cardiac rupture in transgenic mice overexpressing FrzA. Circulation. 2003; 108:2282–2289. [PubMed: 14581414]
10. Kobayashi K, Luo M, Zhang Y, Wilkes DC, Ge G, Grieskamp T, Yamada C, Liu T-C, Huang G, Basson CT, Kispert A, Greenspan DS, Sato TN. Secreted Frizzled-related protein 2 is a procollagen C proteinase enhancer with a role in fibrosis associated with myocardial infarction. Nat Cell Biol. 2009; 11:46–55. [PubMed: 19079247]
11. Oerlemans MIFJ, Goumans M-J, Van Middelaar B, Clevers H, Doevendans PA, Sluijter JPG. Active Wnt signaling in response to cardiac injury. Basic Res Cardiol. 2010; 105:631–641. [PubMed: 20373104]
12. Aisagbonhi O, Rai M, Ryzhov S, Atria N, Feoktistov I, Hatzopoulos AK. Experimental myocardial infarction triggers canonical Wnt signaling and endothelial-to-mesenchymal transition. Dis Model Mech. 2011; 4:469–483. [PubMed: 21324930]
13. Duan J, Gherghe C, Liu D, Hamlett E, Srikantha L, Rodgers L, Regan JN, Rojas M, Willis M, Leask A, Majesky M, Deb A. Wnt1/βcatenin injury response activates the epicardium and cardiac fibroblasts to promote cardiac repair. EMBO J. 2012; 31:429–442. [PubMed: 22085926]
14. He W, Zhang L, Ni A, Zhang Z, Mirotsou M, Mao L, Pratt RE, Dzau VJ. Exogenously administered secreted frizzled related protein 2 (Sfrp2) reduces fibrosis and improves cardiac function in a rat model of myocardial infarction. Proc Natl Acad Sci US A. 2010; 107:21110–5.
15. Daskalopoulos EP, Hermans KC, Janssen BJ, Blankesteijn WM. Targeting the Wnt/frizzled signaling pathway after myocardial infarction: a new tool in the therapeutic toolbox? Trends Cardiovasc Med. 2013; 23:121–7. [PubMed: 23266229]
16. Armstrong DD, Esser KA. Wnt/beta-catenin signaling activates growth-control genes during overload-induced skeletal muscle hypertrophy. Am J Physiol Cell Physiol. 2005; 289:C853–859. [PubMed: 15888552]
17. Bujak M, Frangogiannis NG. The role of TGF-β signaling in myocardial infarction and cardiac remodeling. Cardiovasc Res. 2007; 74:184–195. [PubMed: 17109837]
18. Subramaniam A, Jones WK, Gulick J, Wert S, Neumann J, Robbins J. Tissue-specific regulation of the alpha-myosin heavy chain gene promoter in transgenic mice. J Biol Chem. 1991; 266:24613–24620. [PubMed: 1722208]
19. van den Bos EJ, Mees BME, de Waard MC, de Crom R, Duncker DJ. A novel model of cryoinjury-induced myocardial infarction in the mouse: a comparison with coronary artery ligation. Am J Physiol Heart Circ Physiol. 2005; 289:H1291–H1300. [PubMed: 15863462]
20. van Amerongen MJ, Harmsen MC, Petersen AH, Popa ER, van Luyn MJA. Cryoinjury: a model of myocardial regeneration. Cardiovasc Pathol. 2008; 17:23–31. [PubMed: 18160057]

21. Spinale FG, Coker ML, Heung LJ, Bond BR, Gunasinghe HR, Etoh T, Goldberg AT, Zellner JL, Crumbley AJ. A matrix metalloproteinase induction/activation system exists in the human left ventricular myocardium and is upregulated in heart failure. Circulation. 2000; 102:1944–1949. [PubMed: 11034943]
22. Chan D, Ng LL. Biomarkers in acute myocardial infarction. BMC Med. 2010; 8:34. [PubMed: 20529285]
23. Yabluchanskiy A, Ma Y, Iyer RP, Hall ME, Lindsey ML. Matrix metalloproteinase-9: Many sides of function in cardiovascular disease. Physiology. 2013; 28:391–403. [PubMed: 24186934]
24. Omland T, Aakvaag A, Bonarjee VV, Caidahl K, Lie RT, Nilsen DW, Sundsfjord JA, Dickstein K. Plasma brain natriuretic peptide as an indicator of left ventricular systolic function and long-term survival after acute myocardial infarction. Comparison with plasma atrial natriuretic peptide and N-terminal proatrial natriuretic peptide. Circulation. 1996; 93:1963–1969. [PubMed: 8640969]
25. de Lemos JA, Morrow DA, Bentley JH, Omland T, Sabatine MS, McCabe CH, Hall C, Cannon CP, Braunwald E. The prognostic value of B-type natriuretic peptide in patients with acute coronary syndromes. N Engl J Med. 2001; 345:1014–1021. [PubMed: 11586953]
26. Jho E, Zhang T, Domon C, Joo C-K, Freund J-N, Costantini F. Wnt/beta-catenin/Tcf signaling induces the transcription of Axin2, a negative regulator of the signaling pathway. Mol Cell Biol. 2002; 22:1172–1183. [PubMed: 11809808]
27. Lustig B, Jerchow B, Sachs M, Weiler S, Pietsch T, Karsten U, van de Wetering M, Clevers H, Schlag PM, Birchmeier W, Behrens J. Negative feedback loop of Wnt signaling through upregulation of conductin/axin2 in colorectal and liver tumors. Mol Cell Biol. 2002; 22:1184–1193. [PubMed: 11809809]
28. Behrens J, Von Kries JP, Kühl M, Bruhn L, Wedlich D, Grosschedl R, Birchmeier W. Functional interaction of beta-catenin with the transcription factor LEF-1. Nature. 1996; 382:638–642. [PubMed: 8757136]
29. Chen B, Dodge ME, Tang W, Lu J, Ma Z, Fan C-W, Wei S, Hao W, Kilgore J, Williams NS, Roth MG, Amatruda JF, Chen C, Lum L. Small molecule-mediated disruption of Wnt-dependent signaling in tissue regeneration and cancer. Nat Chem Biol. 2009; 5:100–107. [PubMed: 19125156]
30. Bennett BL, Sasaki DT, Murray BW, O'Leary EC, Sakata ST, Xu W, Leisten JC, Motiwala A, Pierce S, Satoh Y, Bhagwat SS, Manning AM, Anderson DW. SP600125, an anthrapyrazolone inhibitor of Jun N-terminal kinase. Proc Natl Acad Sci US A. 2001; 98:13681–13686.
31. De Vries C, Escobedo JA, Ueno H, Houck K, Ferrara N, Williams LT. The fms-like tyrosine kinase, a receptor for vascular endothelial growth factor. Science. 1992; 255:989–991. [PubMed: 1312256]
32. Millauer B, Wizigmann-Voos S, Schnürch H, Martinez R, Møller NP, Risau W, Ullrich A. High affinity VEGF binding and developmental expression suggest Flk-1 as a major regulator of vasculogenesis and angiogenesis. Cell. 1993; 72:835–846. [PubMed: 7681362]
33. Thurston G, Rudge JS, Ioffe E, Zhou H, Ross L, Croll SD, Glazer N, Holash J, McDonald DM, Yancopoulos GD. Angiopoietin-1 protects the adult vasculature against plasma leakage. Nat Med. 2000; 6:460–463. [PubMed: 10742156]
34. Fuxe J, Tabruyn S, Colton K, Zaid H, Adams A, Baluk P, Lashnits E, Morisada T, Le T, O'Brien S, Epstein DM, Koh GY, McDonald DM. Pericyte requirement for anti-leak action of angiopoietin-1 and vascular remodeling in sustained inflammation. Am J Pathol. 2011; 178:2897–909. [PubMed: 21550017]
35. Semones M, Feng Y, Johnson N, Adams JL, Winkler J, Hansbury M. Pyridinylimidazole inhibitors of Tie2 kiase. Bioorg Med Chem Lett. 2007; 17:4756–5760. [PubMed: 17618114]
36. Tirziu D, Jaba IM, Yu P, Larrivée B, Coon BG, Cristofaro B, Zhuang ZW, Lanahan AA, Schwartz MA, Eichmann A, Simons M. Endothelial Nuclear Factor-κB–Dependent Regulation of Arteriogenesis and Branching. Circulation. 2012; 126:2589–2600. [PubMed: 23091063]
37. Sweet DT, Chen Z, Givens CS, Owens AP 3rd, Rojas M, Tzima E. Endothelial Shc Regulates Arteriogenesis Through Dual Control of Arterial Specification and Inflammation via the Notch and NF-κB Pathways. Circ Res. 2013; 113:32–9. [PubMed: 23661718]

38. Cristofaro B, Shi Y, Faria M, et al. Dll4-Notch signaling determines the formation of native arterial collateral networks and arterial function in mouse ischemia models. Development. 2013; 140:1720–29. [PubMed: 23533173]
39. Lin YZ, Yao SY, Veach RA, Torgerson TR, Hawiger J. Inhibition of nuclear translocation of transcription factor NF-kappa B by a synthetic peptide containing a cell membrane-permeable motif and nuclear localization sequence. J Biol Chem. 1995; 270:14255–14258. [PubMed: 7782278]
40. Andrae J, Gallini R, Betsholtz C. Role of platelet-derived growth factors in physiology and medicine. Genes Dev. 2008; 22:1276–1312. [PubMed: 18483217]
41. Pfosser A, El-Aouni C, Pifsterer I, Dietz M, Globisch F, Stachel G, Trenkwalder T, Pinkenburg O, Horstkotte J, Hinkel R, Sperandio M, Hatzopoulos AK, Boekstegers P, Bals R, Kupatt C. NF kappaB activation in embryonic endothelial progenitor cells enhances neovascularization via PSGL-1 mediated recruitment: novel role for LL37. Stem Cells. 2010; 28:376–385. [PubMed: 20014279]
42. Blankesteijn WM, Van Gijn ME, Essers-Janssen YP, Daemen MJ, Smits JF. Beta-catenin, an inducer of uncontrolled cell proliferation and migration in malignancies, is localized in the cytoplasm of vascular endothelium during neovascularization after myocardial infarction. Am J Pathol. 2000; 157:877–883. [PubMed: 10980127]
43. Augustin HG, Koh GY, Thurston G, Alitalo K. Control of vascular morphogenesis and homeostasis through the angiopoietin-Tie system. Nat Rev Mol Cell Biol. 2009; 10:165–177. [PubMed: 19234476]
44. Cho C-H, Kim KE, Byun J, Jang H-S, Kim D-K, Baluk P, Baffert F, Lee GM, Mochizuki N, Kim J, Jeon BH, McDonald DM, Koh GY. Long-term and sustained COMP-Ang1 induces long-lasting vascular enlargement and enhanced blood flow. Circ Res. 2005; 97:86–94. [PubMed: 15961719]
45. Su H, Takagawa J, Huang Y, Arakawa-Hoyt J, Pons J, Grossman W, Kan YW. Additive effect of AAV-mediated angiopoietin-1 and VEGF expression on the therapy of infarcted heart. Int J Cardiol. 2009; 133:191–197. [PubMed: 18295361]
46. Tao Z, Chen B, Tan X, Zhao Y, Wang L, Zhu T, Cao K, Yang Z, Kan YW, Su H. Coexpression of VEGF and angiopoietin-1 promotes angiogenesis and cardiomyocyte proliferation reduces apoptosis in porcine myocardial infarction (MI) heart. Proc Natl Acad Sci US A. 2011; 108:2064–2069.
47. Taimeh Z, Loughran J, Birks EJ, Bolli R. Vascular endothelial growth factor in heart failure. Nat Rev Cardiol. 2013; 10:519–30. [PubMed: 23856679]
48. Birdsey GM, Shah AV, Dufton N, Reynolds LE, Osuna Almagro L, Yang Y, Aspalter IM, Khan ST, Mason JC, Dejana E, Gottgens B, Hodivala-Dilke K, Gerhardt H, Adams RH, Randi AM. The endothelial transcription factor ERG promotes vascular stability and growth through Wnt/β-catenin signaling. Dev Cell. 2015; 32:82–96. [PubMed: 25584796]
49. Modder UI, Oursler MJ, Khosla S, Monroe DG. Wnt10b activates the Wnt, Notch, and NFkB pathways in U2OS osteosarcoma cells. J Cell Biochem. 2011; 112:1392–1402. [PubMed: 21321991]
50. Zhang Y, Tomann P, Andl T, Gallant NM, Huelsken J, Jerchow B, Birchmeier W, Paus R, Piccolo S, Mikkola ML, Morrissey EE, Overbeek PA, Scheidereit C, Millar SE, Schmidt-Ullrich R. Reciprocal requirements for EDA/EDAR/NF-kappaB and Wnt/beta-catenin signaling pathways in hair follicle induction. Dev Cell. 2009; 17:49–61. [PubMed: 19619491]
51. Heallen T, Zhang M, Wang J, Bonilla-Claudio M, Klysik E, Johnson RL, Martin JF. Hippo pathway inhibits Wnt signaling to restrain cardiomyocyte proliferation and heart size. Science. 2011; 332:458–61. [PubMed: 21512031]
52. Senyo SE, Steinhauser ML, Pizzimenti CL, Yang VK, Cai L, Wang M, Wu TD, Guerquin-Kern JL, Lechene CP, Lee RT. Mammalian heart renewal by pre-existing cardiomyocytes. Nature. 2013; 493:433–496. [PubMed: 23222518]
53. Fioret BA, Heimfeld JD, Paik DT, Hatzopoulos AK. Endothelial cells contribute to generation of adult ventricular myocytes during cardiac homeostasis. Cell Rep. 2014; 8:229–241. [PubMed: 25001281]

54. Ubil E, Duan J, Pillai ICL, Rosa-Garrido M, Wu Y, Bargiacchi F, Lu Y, Stanbouly S, Huang J, Rojas M, Vondriska TM, Stefani E, Deb A. Mesenchymal-endothelial transition contributes to cardiac neovascularization. Nature. 2014; 514:585–590. [PubMed: 25317562]

55. Mirotsou M, Zhang Z, Deb A, Zhang L, Gnecchi M, Noiseux N, Mu H, Pachori A, Dzau VJ. Secreted frizzled related protein 2 (Sfrp2) is the key Akt-mesenchymal stem cell-released paracrine factor mediating myocardial survival and repair. Proc Natl Acad Sci US A. 2007; 104:1643–1648.

56. Hahn JY, Cho HJ, Bae JW, Yuk HS, Kim KI, Park KW, Koo BK, Chae IH, Shin CS, Oh BH, Choi YS, Park YB, Kim HS. Beta-catenin overexpression reduces myocardial infarct size through differential effects on cardiomyocytes and cardiac fibroblasts. J Biol Chem. 2006; 281:30979–89. [PubMed: 16920707]

57. Clevers H, Loh KM, Nusse R. An integral program for tissue renewal and regeneration: Wnt signaling and stem cell control. Science. 2014; 346:1248012. [PubMed: 25278615]

58. Paik, DT.; Hatzopoulos, AK. Wnt signaling in regulation of stem cells. In: Ao, A.; Hao, J.; Hong, CC., editors. Chemical Biology in Regenerative Medicine: Bridging Stem Cells and Future Therapies. John Wiley & Sons, Ltd; Chichester, UK: 2014.

59. Abdul-Ghani M, Dufort D, Stiles R, De Repentigny Y, Kothary R, Megeney LA. Wnt11 promotes cardiomyocyte development by caspase-mediated suppression of canonical Wnt signals. Mol Cell Biol. 2011; 31:163–178. [PubMed: 21041481]

Novelty and Significance

What Is Known?

- Angiogenesis and fibrosis are launched simultaneously during scar tissue formation after myocardial infarction.
- Canonical Wnt signaling is activated within the infarct zone in blood-vessel-forming endothelial cells and collagen-producing myofibroblasts.
- Wnt proteins are induced after myocardial infarction, but their roles in cardiac repair processes are not known.

What New Information Does This Article Contribute?

- The canonical Wnt signaling ligand Wnt10b is stored in the intercalated discs of adult cardiomyocytes and induced in the border zone of the infarct.
- Wnt10b regulates canonical Wnt and NF-κB signaling activation in multiple cell types that take part in the injury repair process.
- Overexpression of Wnt10b in the heart promotes formation of blood vessels and cardiomyocytes, attenuates fibrosis, and preserves left ventricular function after injury.

Despite considerable progress in thrombolytics and percutaneous interventions to restore circulation after myocardial infarction, we have no means to improve the natural healing processes of the heart with the goal of preserving ventricular function and prevent heart failure. We discovered that the canonical Wnt ligand Wnt10b is highly induced in peri-infarct cardiomyocytes after injury, at the onset of scar tissue formation. To study the effects of Wnt10b on the cardiac tissue repair process, we generated a transgenic αMHC-Wnt10b mouse that overexpresses Wnt10b in cardiomyocytes. We found that αMHC-Wnt10b mice show robust formation of blood vessels and cardiomyocytes, less fibrosis, and better preserved ventricular output after acute injury as compared to wild-types. Wnt10b induces endothelial cell proliferation via canonical Wnt signaling activation and stimulates arteriole formation in NF-κB-dependent manner. Our findings suggest Wnt10b has the potential to enhance cardiac tissue repair and regeneration and may lead to novel therapeutic strategies to improve ventricular function after injury.

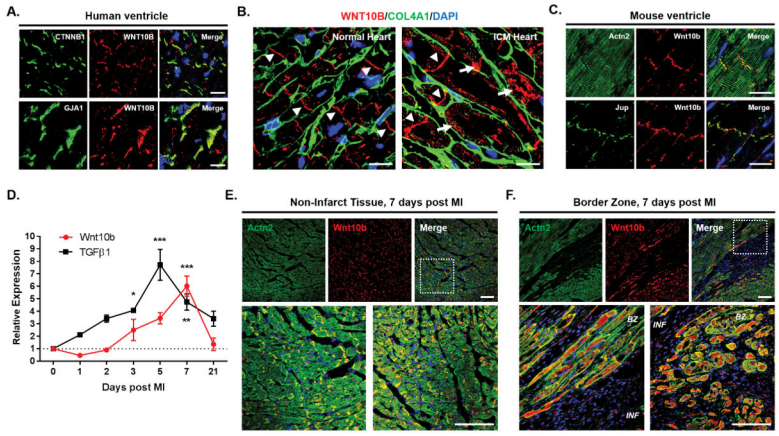

Figure 1. Wnt10b is expressed in cardiomyocytes and induced in chronic and acute cardiac injury

(A) Localization of WNT10B protein in the normal adult human ventricular tissue. IF for WNT10B (red), β-catenin (CTNNB1, top, green) and connexin-43 (GJA1, bottom, green) illustrates localization of WNT10B in the intercalated discs of cardiomyocytes. Scale bars, 20 μm. (**B)** Aberrant accumulation of WNT10B (red) in the cytoplasm of cardiomyocytes (arrows) in ischemic cardiomyopathy (ICM) patients (right), in addition to its localization in the intercalated discs (arrowheads). Normal human heart (left) shown as control. Collagen IV (COL4AI, green) antibody staining of basal membranes outlines borders between cardiomyocytes. Scale bars, 20 μm. (**C)** Localization of Wnt10b in cardiomyocytes of normal adult mouse ventricular tissue. IF for α-Actinin (Actn2, top, green) and plakoglobin (Jup, bottom, green) shows localization of Wnt10b (red) in the intercalated discs. Scale bars, 20 μm. (**D)** *Wnt10b* and *Tgf-β1* mRNA expression by qPCR analysis at sequential time points post experimental myocardial infarction (MI) in mouse hearts. *Wnt10b* levels peak at day 7 after MI, during granulation tissue formation. * $P < 0.05$; ** $P < 0.01$; *** $P < 0.001$. One-way ANOVA with Dunnett's multiple comparisons test. N≥3 for all time points. All data are means ± SEM. (**E)** Wnt10b remains associated with cardiomyocyte junctions in distal, non-infarcted, areas of mouse ventricle 7 days post MI. (**F)** Wnt10b expression (red) is induced and becomes pervasive in the cytoplasm of cardiomyocytes (stained in green for Actn2) in the border zone of mouse hearts 7 days post MI. Low (top) and high (bottom) magnification of cardiac tissue is shown. Left bottom panels depict boxed areas on top. Scale bars, 100 μm. BZ=border zone, INF=infarct tissue. All tissue sections were counter-stained with DAPI (blue) to mark cellular nuclei.

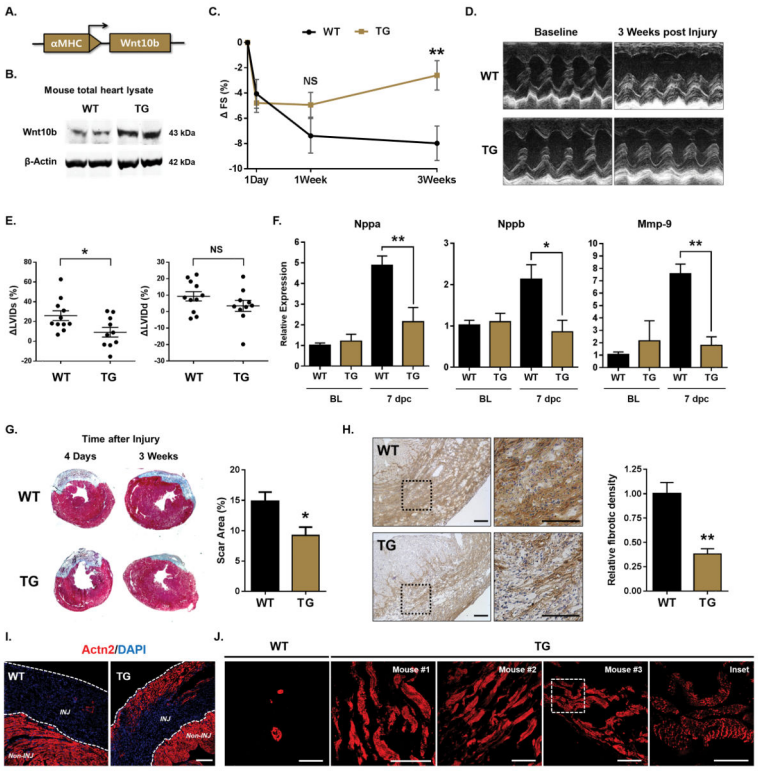

Figure 2. Wnt10b gain-of-function improves ventricular function after injury

(**A**) Schematic drawing of the *αMHC-Wnt10b* transgene (TG). (**B**) Western blot analysis of protein samples isolated from total cardiac tissue shows higher Wnt10b protein levels in TG hearts compared to wild types (WT). β-actin served as loading control. Molecular weights are indicated in kilodaltons (kDa). (**C**) Fractional shortening percentage changes at 1 day, 1 week and 3 weeks after cryoinjury show that cardiac function recovers over time in TG mice, whereas it deteriorates in WT controls. WT N=10, TG N=11. (**D**) Representative M-mode echocardiograms at baseline and 3 weeks after cryoinjury demonstrate improved ventricular function in TG mice compared to WT counterparts 3 weeks after injury. **(E)** Percentage changes in left ventricular internal dimension in systole (LVIDs) and diastole (LVIDd) 3 weeks post cryoinjury, relative to baseline values, indicate functional recovery in TG mice is primarily due to improved systolic function. WT N=10, TG N=11. (**F**) mRNA analysis by qPCR at baseline (arbitrarily set as value 1 in WT) and 7 days post cryoinjury shows that expression of heart failure predictor genes is attenuated in TG mouse hearts compared to WT. BL=baseline, dpc=days post cryoinjury. N=3–6 mice/group. (**G**) Masson's trichrome staining of ventricle sections 4 days and 3 weeks after cryoinjury (left) and quantification of scar size as percentage of horizontal ventricle area (right). TG and WT mice display similar size of original injury. 3 weeks later, scar size in TG hearts is reduced by approximately 2-fold compared to WTs. N=4 mice per group. (**H**) Immunohistochemistry of Col1A in injured tissue of WT and TG ventricles 3 weeks post cryoinjury shows reduced collagen deposits in TG (left). Boxed areas are shown at higher magnification. Scale bars, 200 μm. Quantification of relative fibrotic density (arbitrarily set as value 1 in WT) based on Col1A staining (right). N=4 mice per group. **(I)** Comparison of Actn2 staining for

cardiomyocytes in WT and TG ventricles 7 days post cryoinjury in low magnification shows the appearance of cardiomyocyte patches in TG. Injury areas between epicardium and healthy tissue are delineated with dashed lines. **(J)** Actn2 staining in WT and TG ventricles 7 days post cryoinjury in high magnification. Images from 3 distinct TG mice display abundant Actn2 staining within scar tissue. Inset (far right) shows sarcomeric structures in $Actn2^{+}$ cells. Scale bar, 200 μm; inset, 50 μm. INJ=injured tissue, Non-INJ=non-injured tissue. * $P < 0.05$; ** $P < 0.01$; NS, not significant, unpaired *t* test. All data are means ± SEM.

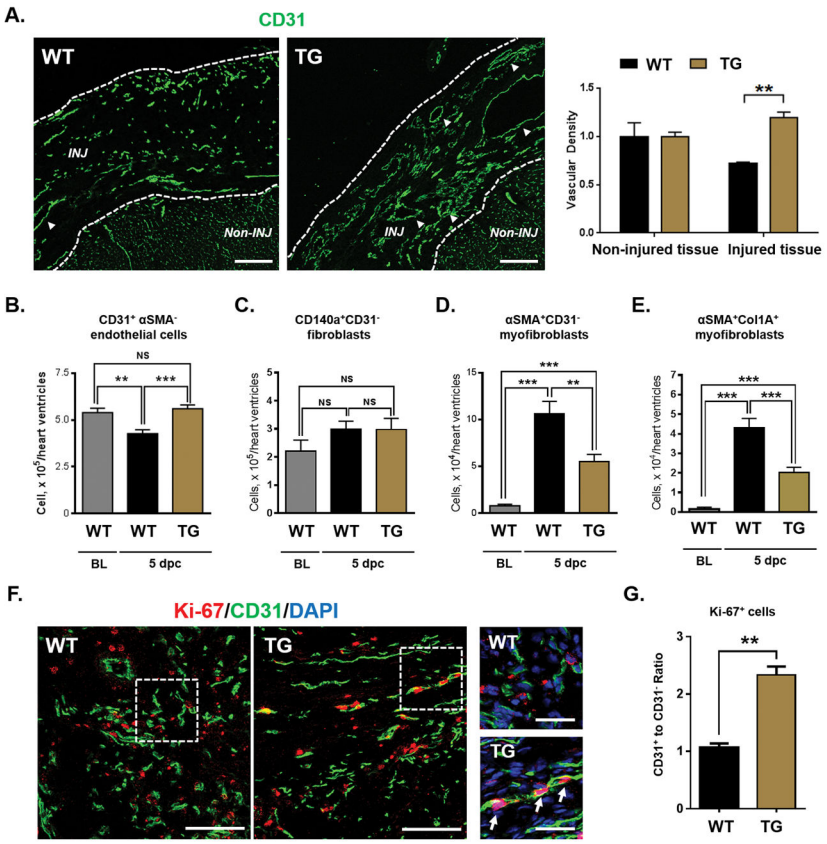

Figure 3. Wnt10b gain-of-function promotes neovascularization and attenuates myofibroblast expansion during cardiac repair after injury

(**A**) Panoramic IF images of CD31 antibody staining (green) in the injury (INJ) and peri-injury (Non-INJ) zones of WT and TG mouse cardiac tissue sections 3 weeks after cryoinjury (left panels). Injury zones between epicardium and non-injured tissue are delineated with dashed lines. The injury zone in WT mice contains mostly micro-capillaries, whereas in TG mice it contains numerous large blood vessels (arrowheads). Scale bars, 200 μm. Quantification of vascular density in non-injury and injury cardiac sections (right) shows scar tissue in TG mice is approximately 2-fold more densely vascularized than WT controls (right). N=3 mice per group. **(B)** Number of $CD31^{+}\alpha SMA^{-}$ endothelial cells, **(C)** $CD140a^{+}CD31^{-}$ fibroblasts, **(D)** $\alpha SMA^{+}CD31^{-}$ myofibroblasts, and **(E)** $\alpha SMA^{+}Col1A^{+}$ myofibroblasts among non-cardiomyocyte $CD45^{-}$ primary cells isolated from WT and TG ventricles, determined by flow cytometry. Cell population numbers from WT ventricles at baseline shown as reference. TG hearts contain higher endothelial cell, equal fibroblast and lower myofibroblast numbers compared to WT 5 days after cryoinjury. BL=baseline, dpc=days post cryoinjury. N=6 mice per group. **(F)** IF analysis with antibodies recognizing Ki-67 (red) and CD31 (green) shows higher numbers of proliferating endothelial cells (arrows) in the injured tissue of TG ventricles compared to WT, 7 days after cryoinjury. Right panels show magnified images from boxed regions on the left and middle panels. Sections were counter-stained with DAPI (blue) to mark cellular nuclei. Scale bar, 100 μm; insets 50 μm. **(G)** Ratio of $Ki\text{-}67^{+}CD31^{+}$ proliferating endothelial cells to $Ki\text{-}67^{+}CD31^{-}$ proliferating stromal cells in WT and TG ventricles 5 days post cryoinjury, determined by

flow cytometry. N=3 mice per group. ** $P < 0.01$; *** $P < 0.001$; NS, not significant, unpaired *t* test. All data are means ± SEM.

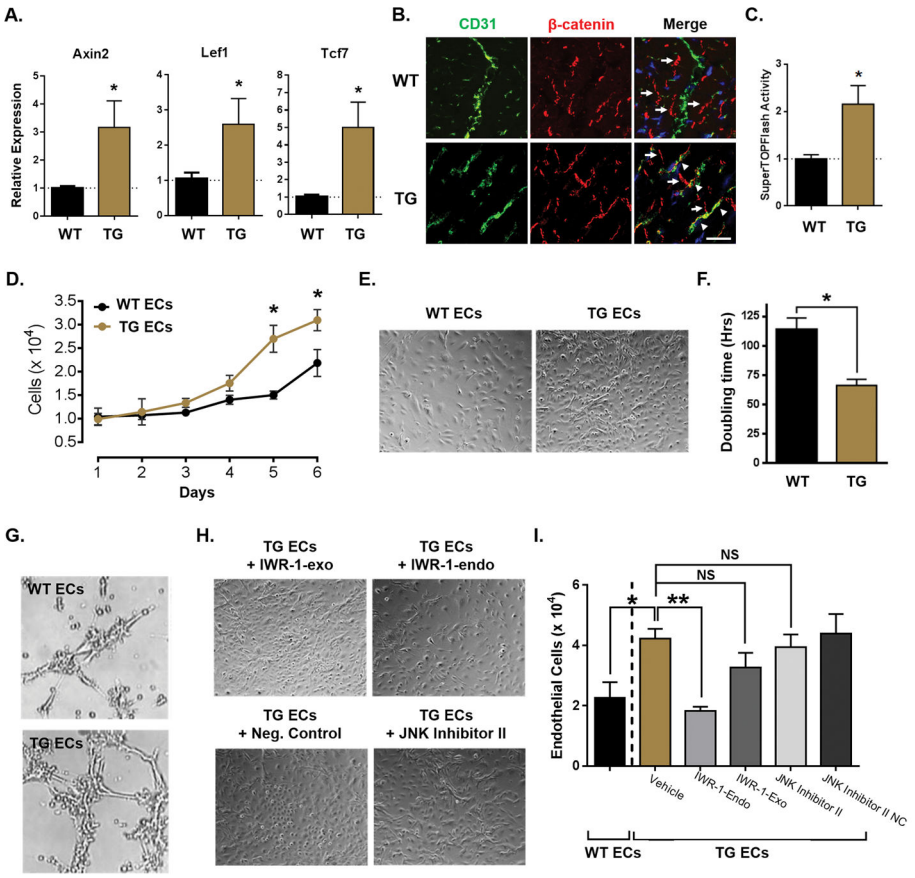

Figure 4. Wnt10b gain-of-function activates canonical Wnt signaling and increases proliferative capacity in resident cardiac endothelial cells

(**A**) qPCR analysis using ventricular RNA samples shows levels of canonical Wnt target genes *Axin2*, *Lef1* and *Tcf7* are increased in TG hearts compared to WT controls. N=3-4 mice per group. (**B**) IF images of CD31 (green), β-catenin (red), and DAPI staining (blue) in cardiac tissue sections. β-catenin is present in the intercalated discs of WT and TG cardiomyocytes (arrows), but shows additional staining in endothelial cells (arrowheads) of TG mice. Scale bar, 20 μm. (**C**) Luciferase reporter assay using the canonical Wnt reporter SuperTOPFlash in primary cardiac endothelial cells isolated from WT and TG ventricles shows TG endothelial cells have activated canonical Wnt signaling. Results obtained in independent cell isolation experiments from 3 mice per group. **(D)** Primary cardiac endothelial cells (ECs) were isolated from WT and TG ventricles, seeded, grown in culture for 6 days and counted. Endothelial cells isolated from TG ventricles show higher growth than WT. Results obtained in independent cell isolation experiments from 3 mice per group. **(E)** Images of isolated endothelial cells from WT and TG hearts at day 5 in culture. Endothelial cell cultures from TG mice are denser than those from WT controls. **(F)** Doubling time of cardiac primary endothelial cells isolated from TG mice is 2-fold higher than the corresponding WT controls. N=3 mice per group. **(G)** Tube formation assay on GFR Matrigel shows cardiac endothelial cells from TG ventricles form more tubes than WT controls. **(H)** Cardiac endothelial cells from TG ventricles were cultured with canonical Wnt inhibitor (IWR-1-endo, 1 μM, top right) and its negative control counterpart (IWR-1-exo, 1

μM, top left) as well as with JNK inhibitor II (1 μM, bottom right) and its negative control counterpart (1 μM, bottom left) during the entire duration of culture. Canonical Wnt inhibition blocks endothelial cell growth, but JNK inhibition has no effect. **(I)** Quantification of endothelial cells for each group (in panel G) counted at day 5 of culture. Cells isolated from WT ventricles served as baseline control. Results obtained in independent cell isolation experiments from 3 mice per group. * $P < 0.05$; ** $P < 0.01$; NS, not significant, unpaired *t* test. All data are means ± SEM.

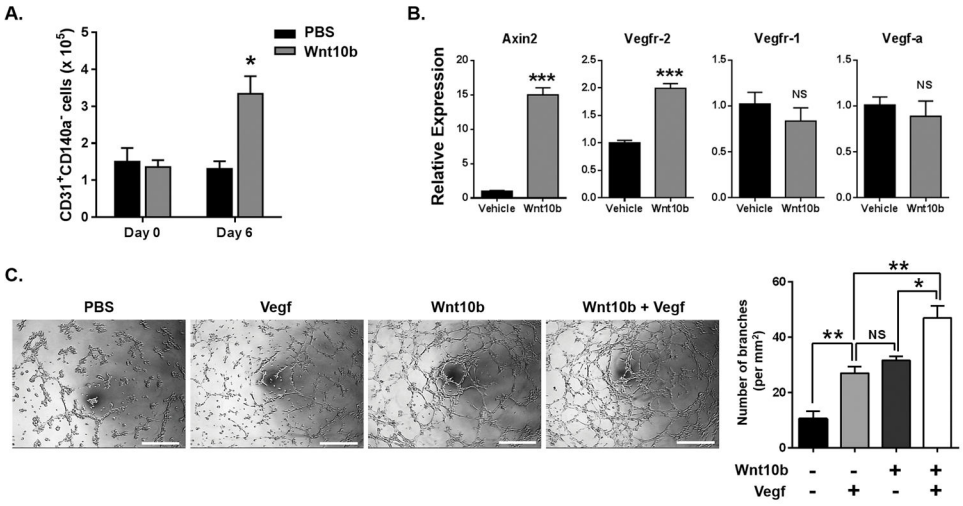

Figure 5. Wnt10b stimulates endothelial cell growth directly and in synergy with VEGF

(**A**) Growth of primary cardiac endothelial cells, $CD31^{+}CD140a^{-}$, isolated from 4 week-old WT ventricles in presence of PBS as vehicle control or Wnt10b protein (300 ng/ml). At day 6, cultures treated with Wnt10b exhibit increased numbers of $CD31^{+}CD140a^{-}$ cells counted by flow cytometry. Results obtained in independent cell isolation experiments from 3 mice per group. **(B)** qPCR analysis shows that Wnt10b induces *Axin2* and *Vegfr-2* in microvascular cardiac endothelial cells (MCEC-1), but it has no effect on *Vegfr-1* and *Vegf-a* expression. **(C)** Wnt10b promotes branching morphogenesis and synergizes with VEGF165 (10 ng/ml) in MCEC-1 cells on GFR Matrigel (left panels). Total number of branches per 1 mm^2 field (right). Results obtained in independent cell isolation experiments from 3 mice per group. * $P < 0.05$; ** $P < 0.01$; *** $P < 0.001$; NS, not significant, unpaired *t* test in panel A and B, one-way ANOVA with Bonferroni's multiple comparisons test in panel C. All data are means ± SEM.

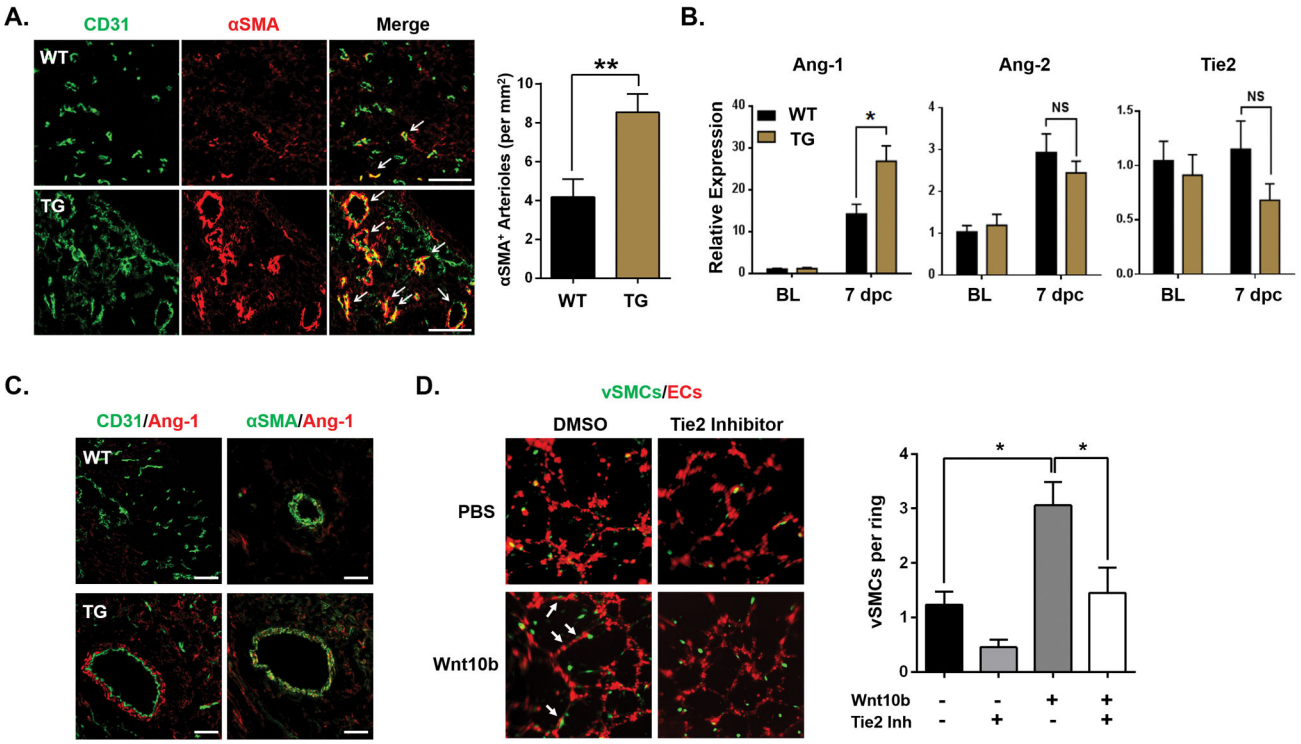

Figure 6. Wnt10b enhances blood vessel stabilization by induction of Angiopoietin-1 and Tie2 signaling

(A) IF images of CD31 (green) and αSMA (red) antibody staining in the scar areas of WT and TG mouse hearts 3 weeks post cryoinjury show Wnt10b promotes formation of stable blood vessels with recruitment of αSMA^+ smooth muscle cells (left). Scale bar, 100 μm. Quantification of the number of αSMA^+ vessels shows that scar areas in TG hearts have 2-fold more arterioles than WT controls. N=3 mice per group. **(B)** qPCR analysis shows *Ang-1* expression 1 week after cryoinjury is enhanced by 2-fold in TG ventricles, as compared to WT controls. In contrast, Ang-2 induction levels are, whereas Tie2 receptor expression remains unchanged after injury in both groups. N=3–4 mice per group. **(C)** IF images of CD31 (green, left), αSMA (green, right), and Ang-1 (red) antibody staining in the injury areas of WT and TG mouse hearts 1 week after cryoinjury shows higher levels of Ang-1 expression in perivascular cells of TG cardiac tissue sections as compared to WT controls. **(D)** Co-culture assay of cardiac endothelial cells (ECs) stained with DiD (red) and vascular smooth muscle cells (vSMCs) stained with DiO (green) on GFR Matrigel to monitor migration and ensheathment of endothelial tubes by vSMCs in the absence of presence of Wnt10b (300 ng/ml) and/or Tie2 Kinase Inhibitor (1 μM). Number of vSMCs per ring counts are shown on the right. N=3–5 wells counted per group. * $P < 0.05$; ** $P < 0.01$; NS, not significant, unpaired *t* test. All data are means ± SEM.

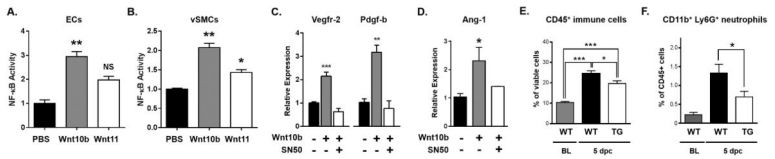

Figure 7. Wnt10b induction of angiogenic and arteriogenic factors depends on activation of NF-κB signaling in endothelial and smooth muscle cells

(A,B) Luciferase activity assay in pNF-κB-luc-plasmid-transfected endothelial cells MCEC-1 (A) and smooth muscle cells MOVAS (B) treated with vehicle (PBS), Wnt10b (300 ng/ml) or Wnt11 (300 ng/ml). Wnt10b activates NF-κB signaling in both cell types. **(C,D)** Wnt10b induction of *Vegfr-2* and *Pdgf-b* in MCEC-1 (C) and *Ang-1* in MOVAS (D) is blocked by the NF-κB inhibitor SN-50 (50 μg/ml). **(E,F)** Flow cytometry based quantification of $CD45^+$ immune cells (E) among viable non-cardiomyocytes and $CD11b^+Ly6G^+$ neutrophils (F) among $CD45^+$ cells isolated from WT and TG ventricles 5 days post cryoinjury (dpc) shows immune cell infiltration is attenuated in TG hearts. Cell populations from WT ventricles at baseline used as reference. N=4–6 mice per group. * $P < 0.05$; ** $P < 0.01$; *** $P < 0.001$; NS, not significant, unpaired *t* test. All data are means ± SEM.

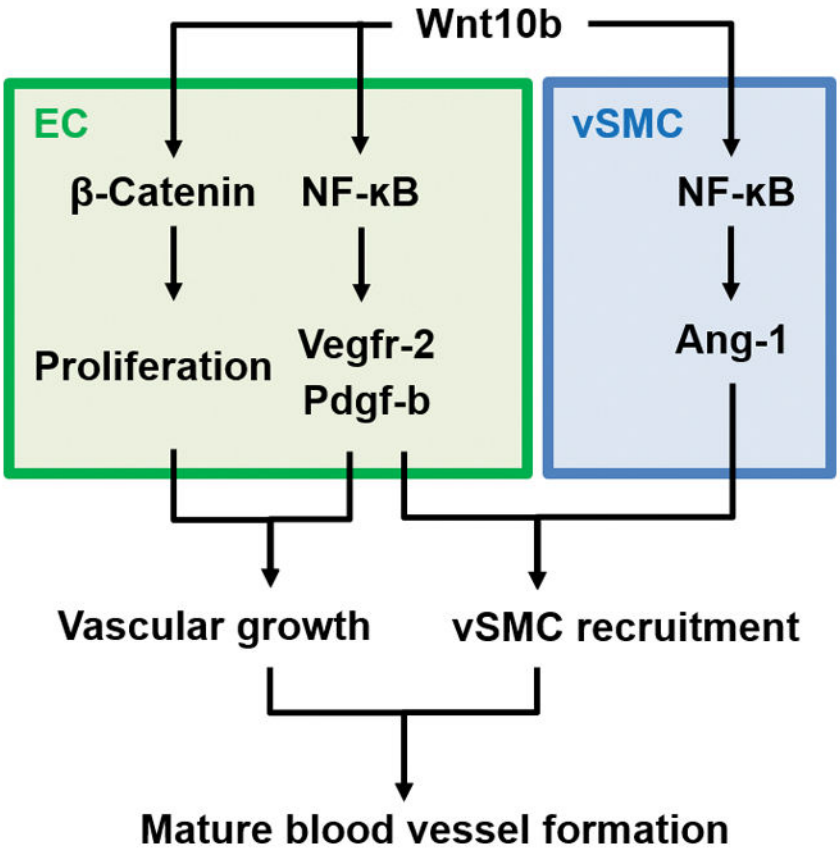

Figure 8. Model of Wnt10b gain-of-function effects on arteriole formation in the injured heart

Wnt10b coordinates blood vessel growth and stability by a) activation of canonical Wnt/β-catenin signaling to stimulate endothelial cell proliferation, and b) NF-κB-dependent induction of Vegfr-2 and Pdgf-b in endothelial cells (EC) and Ang-1 in vascular smooth muscle cells (vSMC) to further promote vascular growth, as well as vSMC recruitment.